

Ultra-fast Microwave Synthesis of ZnO Nanowires and their Dynamic Response Toward Hydrogen Gas

Ahsanulhaq Qurashi · N. Tabet · M. Faiz ·
Toshinari Yamzaki

Received: 12 February 2009 / Accepted: 6 April 2009 / Published online: 25 April 2009
© to the authors 2009

Abstract Ultra-fast and large-quantity (grams) synthesis of one-dimensional ZnO nanowires has been carried out by a novel microwave-assisted method. High purity Zinc (Zn) metal was used as source material and placed on microwave absorber. The evaporation/oxidation process occurs under exposure to microwave in less than 100 s. Field effect scanning electron microscopy analysis reveals the formation of high aspect-ratio and high density ZnO nanowires with diameter ranging from 70 to 80 nm. Comprehensive structural analysis showed that these ZnO nanowires are single crystal in nature with excellent crystal quality. The gas sensor made of these ZnO nanowires exhibited excellent sensitivity, fast response, and good reproducibility. Furthermore, the method can be extended for the synthesis of other oxide nanowires that will be the building block of future nanoscale devices.

Keywords ZnO · Microwave synthesis · Nanowires · FESEM · TEM · XPES · H₂ gas sensor

Introduction

Fabrication of nanowires has received remarkable attention as these one dimensional (1D) nanostructures provide an ideal system to investigate the dependence of transport

properties on size confinement [1]. Nanowires/nanorods are also expected to play an important role as active components or interconnects in fabricating nanoscale electronics and optoelectronics [2–6]. Zinc oxide (ZnO), a wide band-gap (3.37 eV) semiconductor, is a potentially important material. The naturally high surface-to-volume ratio of quasi 1D ZnO nanowires has made it a contender for chemical and biological sensors. In order to explore these applications, availability in large quantities is necessary. In this regard, various synthesis methods have been explored to fabricate ZnO nanowires, most of which are based on physical and chemical techniques; such as chemical vapor transport and condensation processes, metal-organic chemical vapor deposition, anodic alumina membrane templates, aqueous solution process, nonhydrolytic sol–gel processes, pulsed laser deposition, etc. [7–13]. All these methods mentioned above, however, have the disadvantages of low productivity or severe impurities from their employed assistant, so called catalyst or precursor, which bring about discomfort for their real nanodevice applications. Another limitation is the high production cost due to the complex equipment, long processing time and low growth rate. There is still an underlying question of how to scale-up nanoscale production using these approaches. In this regard, microwave heating is relatively new technique for large-scale nanowire processing which is different from existing conventional process.

Hydrogen is a hopeful potential fuel for cars, buses, and other vehicles and can be transformed into electricity in fuel cells. It is also used in medicine and space exploration as well as in the production of industrial chemicals and food products. Safety is an important issue when using the hydrogen. An explosive mixture can form if hydrogen leaks into the air from a tank or valve, posing a hazard to

A. Qurashi (✉) · T. Yamzaki
Department of Engineering, Toyama University, 3190 Gofuku,
Toyama 930-8555, Japan
e-mail: ahsanulhaq06@gmail.com

N. Tabet · M. Faiz
Surface Science Laboratory, Department of Physics, and Center
of Research Excellence in Nanotechnology, King Fahd
University of Petroleum and Minerals, Dhahran, Saudi Arabia

drivers, equipment operators, or others nearby. The present technology to detect hydrogen has numerous drawbacks which include limited dynamic range, poor reproducibility and reversibility, high power consumption and slow response, etc. Therefore, there is a need to develop new generation of metal oxide-based hydrogen gas sensors with improved performance.

In this work, we present the hydrogen gas sensing properties of ZnO nanowires prepared by a novel one-step ultra-fast microwave assisted method. The results show that the ZnO nanowire gas sensor has reversible response to H₂ gas. The work demonstrates the possibility of developing ZnO-based low-power consumption gas sensors and extending their applications.

Experimental Details

Zinc oxide nanostructures were synthesized using microwave technique. A microwave susceptor was used in a modified domestic microwave oven (2.45 GHz, 1250 W) to rapidly evaporate Zn. The microwave susceptor was prepared by mixing silicon carbide powder with oxide additives. A small hole of 10 mm diameter and 3 mm depth was made at the center of its top face. Small pieces of metallic zinc flakes (2–3 mm in size) were placed in the hole. A glass container was placed at a few centimeters above the absorber to collect the ZnO powder. The temperature of the absorber during exposure to microwaves was monitored with a two-wavelength pyrometer (METI-MQ11) connected to a computer. The set-up is shown in Fig. 1. The temperature increases rapidly and exceeds 1,650 °C in less than 100 s exposures. Massive evaporation

of zinc occurs as the temperature reaches about 1,200 °C giving rise to the formation of a vapor made of ZnO nanostructure that deposit on the inner surface of the glass container placed above the absorber. The crystalline phase and morphological and structural features of the products were investigated by X-ray diffraction (XRD Shimadzu-6000) using Cu K_α (0.15418 nm) radiation, field effect scanning electron microscopy (FESEM JSM-6700F), and high-resolution transmission electron microscopy (TEM TOPCON EM-002B). XPS spectra were recorded by using an Electron Spectrometer (type VG-ESCALAB MKII) equipped with a dual (Mg/Al) X-ray source and an ion gun (type EXO5). We have used the aluminum anode (K_α, 1486.6 eV). Zn 2p, C 1s, and O 1s lines were recorded. The interdigitated Pt electrode was prepared on oxidized silicon substrate. The Pt thin film was sputtered on oxidized silicon substrate. The sputtered Pt thin film was then patterned by photolithography and dry etching. About 30 mg of ZnO nanowires dispersed in ethanol and ultrasonicated. The suspension (nanowires and ethanol) dropped onto the interdigitated Pt electrode (3–5 μm thickness). Hydrogen gas sensing measurements were carried out in a quartz tube furnace. Dry synthetic air was used as a reference gas. The gas flow was monitored by mass-flow controllers. A computerized Agilent 34970A multimeter was used for electrical measurements. The resistance of the samples was determined by measuring the electric current under 10 V potential differences between the two electrodes.

Results and Discussion

Structural Characterization

Large quantities (grams) of ZnO nanopowder were collected from the inner wall of the glass container (Fig. 1). Photographic images of the microwave absorber after exposing for 10 and 25 s to microwave are shown in Fig. 2a, b. Figure 2c shows the large quantity of ZnO nanopowder obtained from a single reaction. Typical FE-SEM images of the as-synthesized ZnO nanowires are displayed in Fig. 3 at different magnifications. It can be observed that the nanowires are grown in high-density and large-scale with few micrometer length and diameter in the range of 70–80 nm.

X-ray diffraction measurements were carried out to examine the crystal structure of these nanowires. Figure 4 shows a typical XRD pattern that was indexed to wurtzite hexagonal structure with lattice parameters $a = 3.247 \text{ \AA}$ and $c = 5.203 \text{ \AA}$ which is consistent with reported data (JCPDS, 79-0206). The average grain size (diameter) was estimated to be about 70 nm using Sherrer's formula.

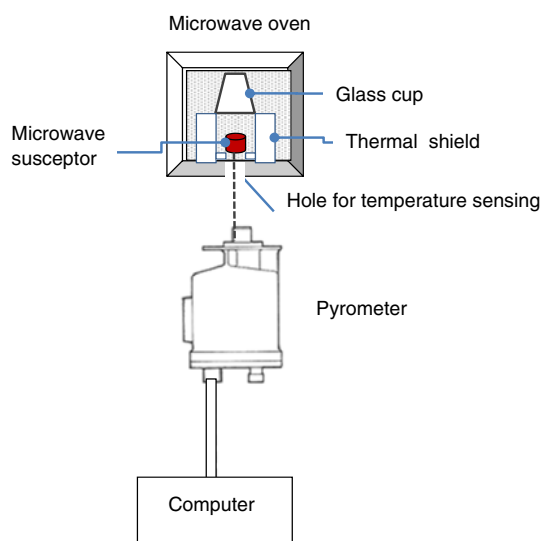


Fig. 1 Schematic diagram of microwave-oven based reaction system used for the synthesis of ZnO nanowires

Fig. 2 Photographic images taken after 10 s **a** and **b** 25 s of exposure to microwave; and **c** ZnO nanopowder in grams quantity

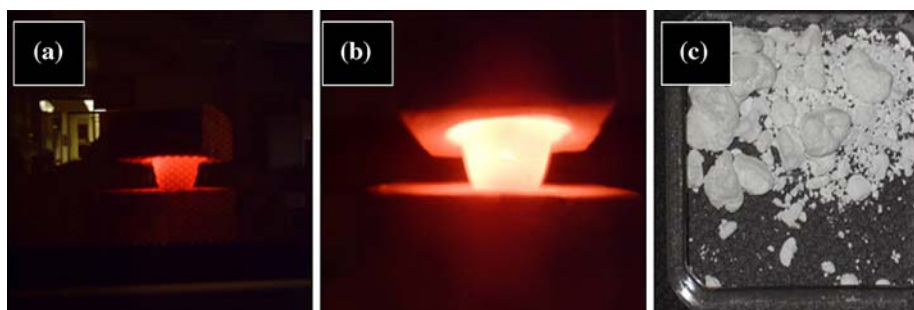


Fig. 3 a–d Low and high magnification FESEM images of ZnO nanowires

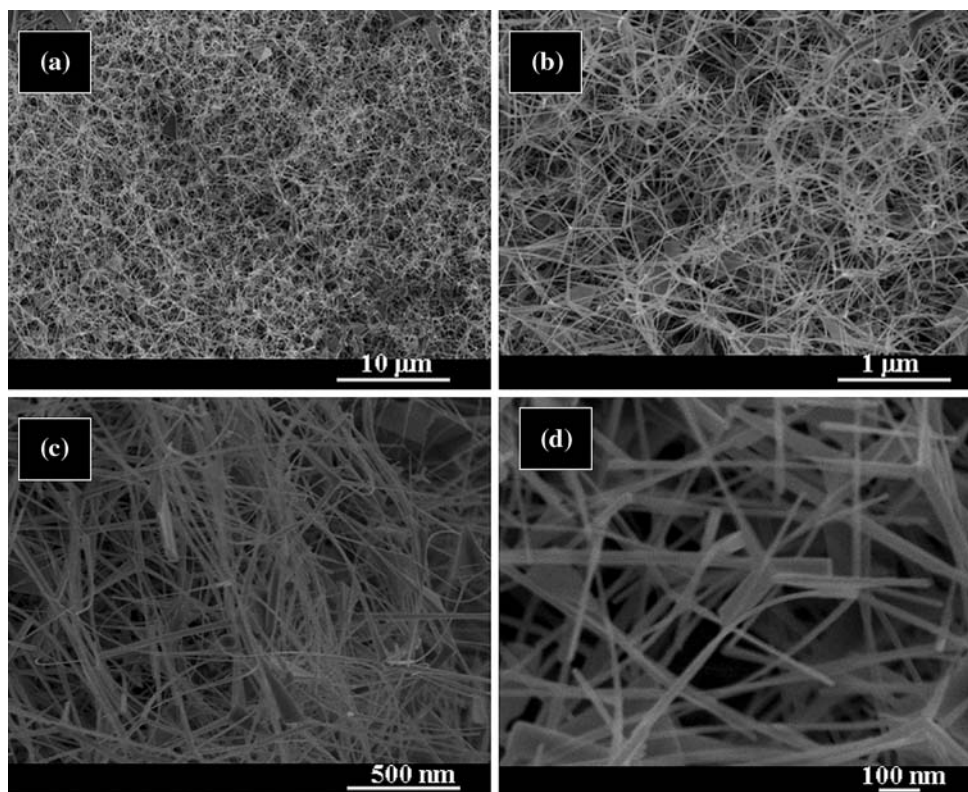


Figure 5a illustrates the morphology of a nanowire of 70 nm diameter as revealed by TEM image. The surface of the nanowires is generally smooth and free from structural dislocations as shown in Fig 5b. The selected area electron diffraction (SAED) pattern in Fig. 5c shows that the ZnO nanowires are single crystalline in nature and grow along the [0001] direction. A high resolution TEM (HRTEM) image in Fig. 5d of the corresponding nanowire is showing the distance of 0.52 nm between two lattice fringes, which represents the (0001) plane of the wurtzite hexagonal ZnO. The XRD and FESEM results are in agreement with the TEM analysis.

Figure 6 shows Zn 2p_{3/2} and O 1s lines of XPS spectra of ZnO nanowires. Charge shift was corrected by fixing the Zn 2p_{3/2} line at 1021.8 eV [14]. The O 1s spectrum shows mainly a peak at 530.4 eV with a small shoulder at about

532.0 eV. The peak is assigned to oxygen atoms bound to Zn in ZnO while the shoulder has been assigned by many authors to the presence of moisture as its binding energy lies between 531.5 eV (OH[−]) and 533 eV (H₂O) [14–16].

Growth Mechanism for the Formation of ZnO Nanowires

Zinc oxide nanowires were grown with the uniform diameter by ultrafast microwave synthesis technique. For the formation of ZnO nanowires Zn metallic particles was used as a source material. Two important factors are responsible for the growth of ZnO nanowires: the formation of crystalline nuclei and axial growth of ZnO nuclei [17]. The formation of nuclei depends on experimental parameters. We used swift microwave synthesis to grow

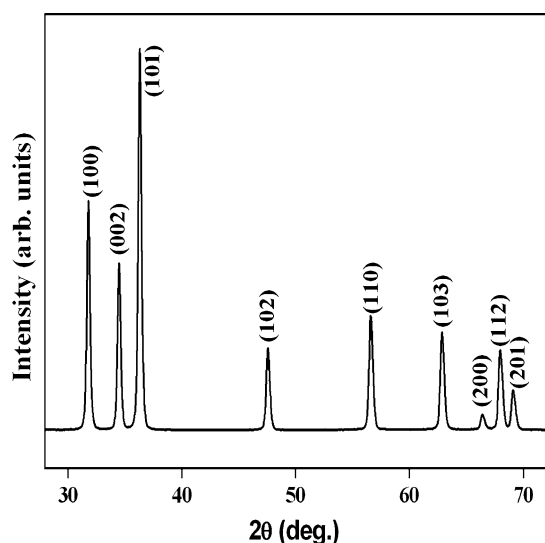
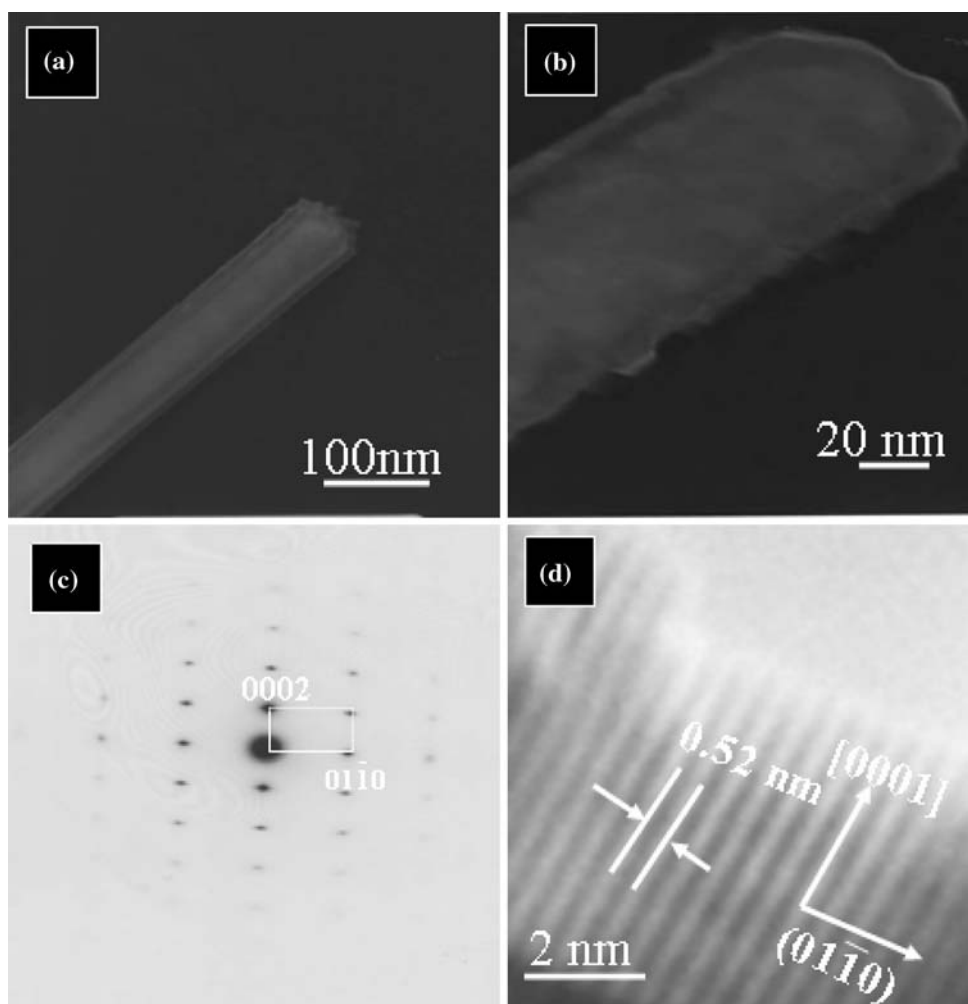


Fig. 4 X-ray diffraction spectrum of ZnO nanowires

1D ZnO nanowires. The Zn particles were easily oxidized into ZnO when temperature surpasses to 419 °C. Owing to the fast oxidation, nanosized crystal nuclei were generated. These crystal nuclei were possibly generating sites for ZnO vapors, and thus the nanowires were most likely grown under the control of ZnO crystal growth habit. With the increase of reaction time and temperature, substantial quantity of ZnO nanowires was formed. ZnO is a polar crystal, where zinc and oxygen atoms are arranged alternatively along the c-axis and the top surface is Zn-terminated [0001] while the bottom surface is oxygen-terminated [000 $\bar{1}$] [18–21]. The top surfaces are Zn-terminated (0001) which are catalytically active, while the bottom surfaces are oxygen-terminated (000 $\bar{1}$) which are chemically inert. Consequently, ZnO crystal grows fast along the direction in which the tetrahedron corners point [18]. The growth along the [0001] direction is dominated over other growth facets. This implies that the c-axis is the

Fig. 5 **a** and **b** Low and high magnification TEM images of ZnO nanowires, **c** Corresponding SAED pattern, and **d** HRTEM



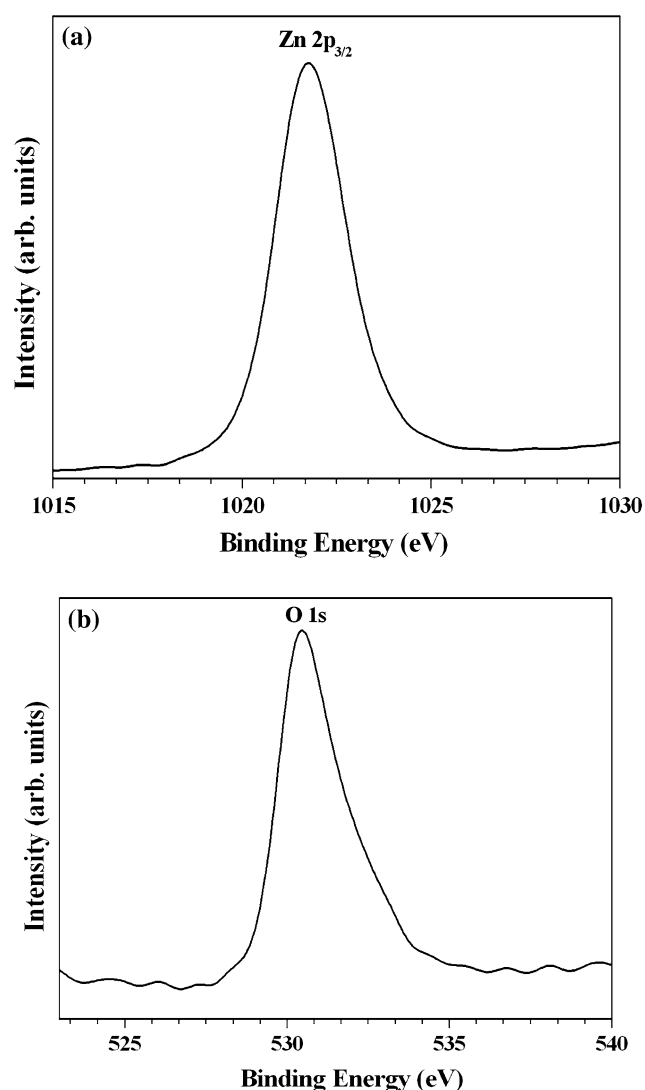
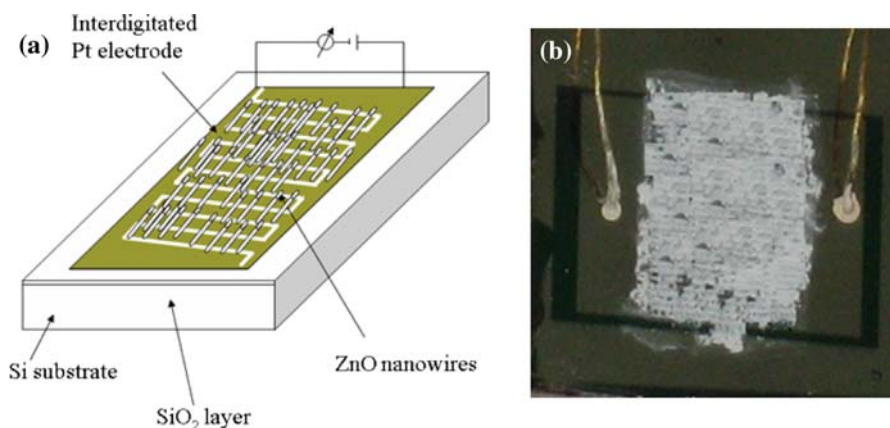


Fig. 6 XPS survey spectrum of ZnO nanowires: **a** Zn 2p_{3/2} and **b** O 1s lines

highest growth direction and the ZnO [0001] has the highest energy of the low-index surface which results in the formation of 1D ZnO nanowires.

Fig. 7 **a** Schematic illustration of the ZnO nanowire gas sensor device. The gap between two Pt fingers is 0.04 mm; **b** photograph of the ZnO nanowire gas sensor. Gas sensor was connected to the measurement circuit using gold wires



Gas Sensing Performance of ZnO Nanowires

Zinc oxide nanowires synthesized by microwave-assisted process possess a large surface-to-volume ratio and high crystal quality. This makes them attractive candidates for gas and chemical sensing applications. Figure 7a illustrates a schematic diagram of the gas sensor device. Figure 7b shows a photograph of the device ready for measurement. Figure 8a shows the resistance response of the ZnO nanowires at 200 °C, as the ambient gas was changed from synthetic air to 500 (0.1%), 1000, and 1500 ppm hydrogen gas. The resistance decreases drastically upon exposure to hydrogen gas, and further decreases by increasing concentration of H₂ from 500 to 1,500 ppm. The resistance recovers its initial value after H₂ elimination, indicating an excellent reproducibility of these ZnO-based gas sensors. The response time for 500 ppm H₂ gas was about 65 s. However, the recovery time was longer (about 148 s). These results are consistent with the expectation of higher relative response based on large surface-to-volume ratio and higher crystal quality of ZnO nanowires. The gas sensing mechanism is based on reversible chemisorption/desorption of hydrogen on the surface of ZnO nanowires. Oxygen is adsorbed on the surface of ZnO nanowire as O[−] or O^{2−} by capturing electrons [22, 23]. The presence of a negative charge on the surface leads to the formation of a depletion region underneath the surface and energy band bending due to the built-in electrical field directed toward the surface. The width of the depletion region is expected to change as the surface charge changes [24–27]. The reduction of the depletion region width as a result of desorption of negative species from ZnO surface was suggested to explain the increase of the excitonic emission of ZnO thin films under UV-illumination [28]. The change of ZnO resistance under exposure to hydrogen gas is still the subject of debate [29]. There are two different processes that could explain the reduction of the resistance of ZnO nanowires when exposed to hydrogen and its recovery after switching back to the initial conditions. First, the

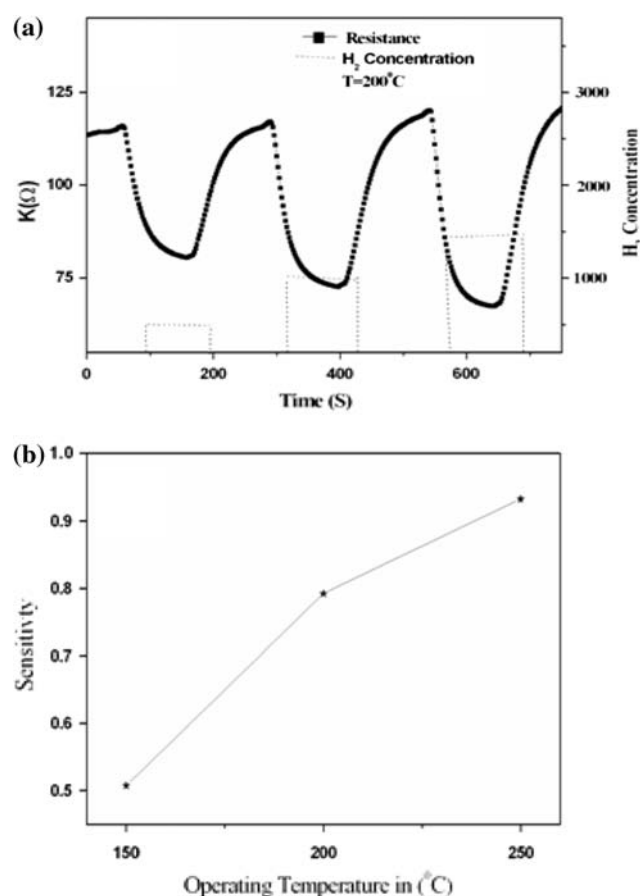
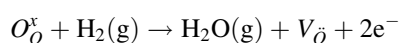


Fig 8 **a** Response of a gas sensor made of ZnO nanowires at 200 °C to H₂ gas at different concentrations. **b** temperature versus sensitivity of ZnO nanowires

atomic hydrogen reacts with the negative oxygen species leading to its desorption and the formation of water molecule. As a result, the negative charge on the surface is reduced and so is the width of the depletion region, the energy band bending, and the corresponding energy barrier. Consequently, the conduction of the regions of the nanowires near the surface increases drastically. The process is very fast as it is controlled by desorption of the oxygen species. When the surface charge is completely removed, further change of the conductivity could occur as a result of the increase of the density of native defects such as the ionized oxygen vacancies which evolve toward the value corresponding to the thermodynamic equilibrium. Hydrogen gas is expected to react with oxygen atoms of ZnO to form water molecules, oxygen vacancies and free electrons in the conduction band. This process can be described by using Kroger and Vink notations as follows:



where, V_O^{\bullet} represents an oxygen vacancy positively ionized twice and O_O^x is an oxygen atom on an oxygen site of ZnO lattice. The above reaction shows that the presence of

hydrogen in the atmosphere leads to the increase of oxygen vacancies that act as donors by increasing the density of free electrons and the conductivity of ZnO nanowires. Our results indicate that ZnO nanowires showed a slow recovery as compared to the fast response to hydrogen exposure. This observation suggests that the adsorption of ionized oxygen species on the surface of ZnO nanowires and the re-establishment of a depletion region is slower than the process of desorption. When the H₂ flow was discontinuous, oxygen molecules again adsorbed onto the ZnO surface and current decreased to the initial value. The decrease of current or recovery is controlled by diffusion and desorption of hydrogen on the surface of nanowires. Thus, the slow recovery is attributed to the desorption process of hydrogen from the nanowire surface and Pt metal surface. Finally, the sensor approached toward the equilibrium state. Figure 8b illustrates the sensitivity of ZnO nanowires at various operating temperatures. The sensitivity increases by increasing the operating temperature. At the operating temperature of 250 °C, the response of nanowires was more prominent than that of the operating temperature 150 °C and 200 °C which can be ascribed to the intensified reaction between the hydrogen and the adsorbed oxygen in the increasing temperature. Further exploration on the electrical properties of ZnO nanowires and their doping effect on the gas sensor response are underway.

Conclusion

In conclusion, single crystal ZnO nanowires were synthesized from high purity Zn metal via an ultra-fast, microwave-assisted process. The major advantage of this technique is its simplicity, low power consumption, fast growth (100 s), and large quantity (in grams) of nanowires. The ZnO nanowires have a wurtzite structure and showed a fast response and high sensitivity to hydrogen gas at 200 °C.

Acknowledgment The authors would like to thank KFUPM for its support. Ahsanulhaq Qurashi is thankful to venture business laboratory of Toyama University for post doctoral fellowship.

References

1. J. Hu, T.W. Odom, C. Leiber, *Acc. Chem. Res.* **32**, 435 (1999). doi:[10.1021/ar9700365](https://doi.org/10.1021/ar9700365)
2. Q. Ahsanulhaq, J.H. Kim, Y.B. Hahn, *Nanotechnology* **18**, 485307 (2007). doi:[10.1088/0957-4484/18/48/485307](https://doi.org/10.1088/0957-4484/18/48/485307)
3. N.K. Reddy, Q. Ahsanulhaq, J.H. Kim, Y.B. Hahn, *Nanotechnology* **18**, 445710 (2007). doi:[10.1088/0957-4484/18/44/445710](https://doi.org/10.1088/0957-4484/18/44/445710)
4. N.K. Reddy, Q. Ahsanulhaq, J.H. Kim, Y.B. Hahn, *Appl. Phys. Lett.* **92**, 043127 (2008). doi:[10.1063/1.2839579](https://doi.org/10.1063/1.2839579)

5. N.K. Reddy, Q. Ahsanulhaq, J.H. Kim, Y.B. Hahn, *Europhys. Lett.* **81**, 38001 (2008). doi:[10.1209/0295-5075/81/38001](https://doi.org/10.1209/0295-5075/81/38001)
6. N.K. Reddy, Q. Ahsanulhaq, Y.B. Hahn, *Appl. Phys. Lett.* **93**, 083124 (2008). doi:[10.1063/1.2975829](https://doi.org/10.1063/1.2975829)
7. S.C. Lyu, Y. Zhang, J.C. Lee, H. Ruh, J.H. Lee, *Chem. Mater.* **15**, 3294 (2003). doi:[10.1021/cm020465j](https://doi.org/10.1021/cm020465j)
8. W.I. Park, D.H. Kim, S.W. Jung, G.C. Yi, *Appl. Phys. Lett.* **80**, 4232 (2003). doi:[10.1063/1.1482800](https://doi.org/10.1063/1.1482800)
9. G.S. Wu, T. Xie, X.Y. Yuan, Y. Li, L. Yang, Y.H. Xia, D.L. Zhang, *Solid State Commun.* **134**, 485 (2005). doi:[10.1016/j.ssc.2005.02.015](https://doi.org/10.1016/j.ssc.2005.02.015)
10. F.D. Zhang, D.L. Sun, L.J. Yin, C.H. Yan, M.R. Wang, *J. Phys. Chem. B* **109**, 8786 (2005). doi:[10.1021/jp050631i](https://doi.org/10.1021/jp050631i)
11. J.M. Zheng, D.L. Zhang, H.G. Li, Z.W. Shen, *Chem. Phys. Lett.* **363**, 123 (2002). doi:[10.1016/S0009-2614\(02\)01106-5](https://doi.org/10.1016/S0009-2614(02)01106-5)
12. J.H. Choi, H. Tabata, T. Kawai, *J. Cryst. Growth* **226**, 493 (2001). doi:[10.1016/S0022-0248\(01\)01388-4](https://doi.org/10.1016/S0022-0248(01)01388-4)
13. Q. Ahsanulhaq, A. Umar, Y.B. Hahn, *Nanotechnology* **18**, 115603 (2007). doi:[10.1088/0957-4484/18/11/115603](https://doi.org/10.1088/0957-4484/18/11/115603)
14. J. Moulder, W.F. Stickle, P.E. Sobol, D.K. Bomben, in *Handbook of X-ray Electron Spectroscopy*, ed. by J. Chastain (Perkin-Elmer, Minnesota, 1992)
15. E. Avallé, E. Santos, A. Leiva, V. Macagno, *Thin Solid Films* **219**, 7 (1992). doi:[10.1016/0040-6090\(92\)90717-P](https://doi.org/10.1016/0040-6090(92)90717-P)
16. J.L. Meng, P.C. Moreira de Sa, P.M. dos Santos, *Appl. Surf. Sci.* **78**, 57 (1994). doi:[10.1016/0169-4332\(94\)90031-0](https://doi.org/10.1016/0169-4332(94)90031-0)
17. C. Yan, J. Liu, F. Liu, J. Wu, K. Gao, D. Xue, *Nanoscale Res. Lett.* **3**, 473 (2008). doi:[10.1007/s11671-008-9193-6](https://doi.org/10.1007/s11671-008-9193-6)
18. C. Yan, D. Xue, *J. Phys. Chem. B* **110**, 25850 (2006). doi:[10.1021/jp0659296](https://doi.org/10.1021/jp0659296)
19. C. Yan, D. Xue, *Electrochem. Commun.* **9**, 1247 (2007)
20. Q. Ahsanulhaq, S.H. Kim, J.H. Kim, Y.B. Hahn, *Mater. Res. Bull.* **43**, 3483 (2008). doi:[10.1016/j.materresbull.2008.01.021](https://doi.org/10.1016/j.materresbull.2008.01.021)
21. Q. Ahsanulhaq, J.H. Kim, N.K. Reddy, Y.B. Hahn, *J. Ind. Eng. Chem.* **14**, 578 (2008). doi:[10.1016/j.jiec.2008.09.001](https://doi.org/10.1016/j.jiec.2008.09.001)
22. T.H. Wang, S.B. Kang, F. Ren, C.L. Tien, W.P. Sadik, P.D. Norton, S.J. Pearton, J. Lin, *Appl. Phys. Lett.* **86**, 243503 (2005). doi:[10.1063/1.1949707](https://doi.org/10.1063/1.1949707)
23. F.J. Chang, H.H. Kuo, C.I. Leu, H.M. Hon, *Sens. Actuators B* **84**, 258 (1994). doi:[10.1016/S0925-4005\(02\)00034-5](https://doi.org/10.1016/S0925-4005(02)00034-5)
24. R.A. Raju, C.N.R. Rao, *Sens. Actuators B* **4**, 305 (1991). doi:[10.1016/0925-4005\(91\)80021-B](https://doi.org/10.1016/0925-4005(91)80021-B)
25. S. Saito, M. Miyayama, K. Kuomoto, H. Yanagida, *J. Am. Ceram. Soc.* **68**, 40 (1985). doi:[10.1111/j.1151-2916.1985.tb15248.x](https://doi.org/10.1111/j.1151-2916.1985.tb15248.x)
26. L.H. Hartnagel, L.A. Dawar, K.A. Jain, C. Jagadish, *Semiconducting Transparent Thin Films* (IOP, Bristol, 1995)
27. O. Lupan, G. Chui, L. Chow, *Microelectron. J.* **38**, 1211 (2007). doi:[10.1016/j.mejo.2007.09.004](https://doi.org/10.1016/j.mejo.2007.09.004)
28. C. Jin, A. Tiwari, J.J.R. Narayan, *Appl. Phys. (Berl)* **98**, 083707 (2005)
29. T.H. Wang, S.B. Kang, F. Ren, C.L. Tien, W.P. Sadik, P.D. Norton, S.J. Pearton, J. Lin, *Appl. Phys. Lett.* **86**, 243503 (2005). doi:[10.1063/1.1949707](https://doi.org/10.1063/1.1949707)